Assessment of the wake effect on the energy production of onshore wind farms using GIS

Stefano Grassi *, Sven Junghans, Martin Raubal

ETH Zurich, Institute of Cartography and Geoinformation, Stefano Franscini Platz 5, 8093 Zurich, Switzerland

HIGHLIGHTS

- Annual energy production of onshore four wind farm estimated with GIS.
- Wake effect, roughness factor and elevation difference of WTs modeled and integrated into GIS.
- Wake effect impact represented with reduced efficiency coefficient (REC).
- Mean annual energy production and capacity factor underestimated of 3.56% and 1.11%.
- Mean REC of wind farm comprised between −0.087 and −0.2.

ARTICLE INFO

ABSTRACT

In this study, we propose a method to estimate the mean annual energy production of a wind farm with a Geographic Information System (GIS). GIS allows for spatial modeling in many fields and has recently been applied in the field of renewable energy. The geographic features of a wind park are represented using spatial data such as topography, land cover, and wind resource. Wind resource layers contain data of the 16 wind directions, in which the wind rose is divided, including the frequency of the wind direction, the mean annual wind speed and the annual Weibull parameters k and C) estimated at 50 m height. The wind turbines are represented by points including information about the roughness of the surrounding terrain. Roughness is calculated within a GIS process that models the variation of the land cover over the year around the wind turbine position. The mean annual energy production is calculated coupling the technical characteristics of the wind turbines models with the wind resource. In addition, the wake effect between wind turbines has been included. A parameter called "reduced efficiency coefficient" has been introduced to assess the impact of the layout of wind farm on the annual energy production in respect to the change of the wind direction. The reduced efficiency coefficient shows that relatively regular wind farm layouts designed for exploiting the wind speed blowing from the prevailing wind direction can cause significant energy losses. In particular, when the wind comes from directions perpendicular to the prevailing one, the wind turbines waste up to 60% of the available energy. The method has been tested, comparing the actual annual energy production of four wind farms in Kansas (U.S.) with the estimated mean annual energy production. The validation demonstrated an average underestimation of 3.56% of the annual energy production and an average underestimation of 1.11% of the capacity factor. The results are encouraging and the developed process enables the quantification of the annual energy production with low uncertainties.

1. Introduction

With the depletion of conventional sources and the increase of global warming, RES have attracted the interest and a more and more significant mass of investments. Among all RES, wind energy has had a growth of 27% in the last five years for a total installed capacity of 230 GW at the end of 2011 [1] with an overall turnover of 50 billion Euro [2].

In order to improve the reliability and thus reduce the uncertainties in investments in the wind energy industry, several efforts have been made in fields such as the improvement of WT efficiency, the development of methods to predict the wind resource and to estimate the wind AEP. With respect to the estimate of

---

Nomenclature

Abbreviation

AEP	annual energy production
AGL	above ground level
ASL	above sea level
DEM	digital elevation model
GIS	Geographic Information System
GW	gigawatt
NREL	National Renewable Energy Laboratory
PPA	power purchase agreement
RES	renewable energy sources
RIX	ruggedness index
WT(s)	wind turbine(s)

Symbols

a	induction factor of a WT
α	constant characteristic of the wake expansion
A	area rotor
A_o	overlapping area between wake of the WT_i and WT_k rotor
A_w	area wake
β	constant characteristic of the wake expansion
C	Weibull Scale coefficient
C_p	power coefficient
C_t	thrust coefficient
CF	capacity factor
γ	availability factor
Δ	difference
ΔLD	distance between two WTs along the wind direction
ΔHD	distance between two WTs perpendicular to the wind direction
Δz	difference of the elevation of two WTs rotors
D	rotor diameter (m)
DW	distance between the center of the WT rotor and the wake
ε	electrical and mechanical losses
φ	angle of the wind direction with respect to the reference
H	hub height (m)
H_{ref}	reference height at which the wind speed is known (m)
K	Weibull Shape factor at the hub height
λ	ratio of the distance x_i between two WTs to the D
μ	frequency

n	number of sectors of the wind rose
n_{30}	number of raster cells in a given area with a slope larger than 30%
n_{all}	total number of raster cells in the area
P	power output of a WT
r	radius
REC	reduced efficiency coefficient
RIX_{wt}	RIX value at the wind turbine location
RIX_m	RIX value at the measurement station
φ	wind direction
U	wind speed
u_{cut-in}	wind speed at which a WT starts producing electricity
$u_{cut-off}$	wind speed at which a WT stops producing electricity
$\bar{u}_H$	wind speed at the hub height (m/s)
$\bar{u}_{ref}$	wind speed at the reference height (m/s)
$\bar{u}_i$	undisturbed inlet wind speed velocity
$\bar{u}_k$	inlet wind speed at the WT in downstream
$\bar{u}_{ik}$	velocity of the wake approaching the WT_k
u_{rated}	wind speed at which a WT reaches the maximum power output
z	WT rotor elevation
z_0	terrain roughness

Subscript

a	at the hub height
Actual	actual AEP
Avail	availability
Cut-in	cut-in wind speed of a WT
Cut-off	cut-off wind speed of a WT
Ref	reference height at which the wind data are known
i	i-WT in upstream
j	number of WT of a wind energy project
loss	losses
k	k-WT in downstream
m	measurement location
predicted	predicted AEP
rated	rated wind speed
ww	with wake included
w/w	without wake
WT	wind turbine

---

the energy production, different models have been developed both for short-term and long-term assessments using statistical and physical approaches.

In this research a method for predicting the AEP of wind farms using a GIS platform has been developed using a physical approach.

A review of previous work is presented in Section 2; in Section 3 the discussion continues with the methodology applied in this process and the characteristics of the data used. Section 4 describes the workflow and in Section 5, the case studies and conclusions are presented.

2. Literature review

Both short-term and long-term energy production estimates are the most important factors that impact the performances, management and profitability of a wind energy project, therefore significant work has been done in the last decades in order to reduce their uncertainties and improve their reliability. The energy production depends on the wind speed prediction and the estimate

of different losses due to the wake effect, mechanical performances of the equipment etc. The wind speed profile is influenced by multiple local obstacles such as topography and land cover and usually varies with height. In addition, the interaction between WTs generates losses and thus further uncertainties in estimating the energy generation. Existing models focus both on the estimate of the wind resource and the energy production of wind farms. The models to estimate the wind energy generation can be divided into two main groups: physical and statistical models. Previous work has widely analyzed and compared these two methods aimed to predict the short- and long-term wind power energy [3] with the scope of identifying which one performs best. The conclusion is that some models are good for short-term predictions while others are more reliable and accurate for long-term predictions. The study finally suggests to develop new technics that adopt more advanced mathematical-based approaches, to combine different physical and statistical models for both in long- and short-term prediction and, finally, to test them on practical applications. A similar study has been carried out to create a benchmark of different models and assessing the uncertainty of the short-term predictions [4]. In other research studies high resolution regional atmospheric systems

have been combined with statistical post-processes in order to improve the accuracy when estimating the short-term wind speed and the wind power at the wind farm location over two areas in Greece [5].

The short-term power predictions (ranging from 1 h up to 72 h) are useful for power system planning, electricity dispatching and trading. The long-term predictions (ranging from months up to years) are useful for planning wind energy projects and prospecting. The work presented in this paper addresses the latter case and in particular the estimate of the AEP using the spatial distribution of the long-term wind speed estimated through long-term observations and integrated in a GIS platform. The spatial wind speed data are represented using GIS vector or raster data.

Initial studies to estimate the AEP of wind farms were simple models based on theoretical assumptions about the WTs and wind characteristics. Probabilistic models of a wind farm have been developed [6] to address the reliability issues considering the stochastic nature of the wind, failure and repair process of wind turbines under certain wind regimes. Biswas et al. [7] proposed a simplified statistical technique for computing the annual energy generation using 12 input variables as input parameters. Assumptions such as 100% availability of the WTs and the theoretical value of the cut-in wind speed are used but they increase the uncertainties in the estimates. With the development of computational tools and techniques further methods have been implemented and applied.

Other studies in the last decades showed how monthly and annual energy production are calculated by coupling the WT characteristics with the Weibull distribution that describes the wind speed distribution over a given time period in one defined location [8] or over a large region [9]. The Weibull distribution is widely used to describe the wind speed pattern at a given site: it is a special case of the Pearson Type III or generalized gamma distribution characterized by two parameters as input data [10,11]. The parameters of the Weibull distribution are used in international standard procedures [12] and estimated using meteorological measurements by applying different statistical methodologies [13] such maximum likelihood, least squares, and method of moments in order to calculate the energy production of wind farms.

Other studies used the same distribution in order to match the WTs with the wind regime at a given site [14] or to estimate the energy potential in a specific location as discussed by Ahmed in [15] for the area close to Hurghada or in different locations in Turkey as demonstrated by Ucar and Balo in [16]. The monthly energy production has been assessed in other studies using three different methodologies [17]: using hourly resolution wind data, monthly wind velocity coupled with the theoretical power curve of WTs and as third method by a simple linear regression calculated over the monthly wind speed and wind power pairs. The Weibull distribution has also been integrated in a complex mathematical process aimed at assessing the uncertainties in the wind energy production estimate [18].

The friction of the terrain, known as aerodynamic roughness factor, which affects the wind profile is often represented by a constant that describes the land cover in a given location independent from the direction and the season [19]. The impact of the roughness on the extrapolation of the wind speed has been addressed for decades starting with theoretical work [20] and continued by investigating the mean and gust wind speeds in the transitional flow regime in inhomogeneous terrains compared to full-scale measurements [21]. In other work, the assessment of the variation of z_0 by year, month and hour of the day, as well as by wind direction, using 1 h wind data measurements in different locations [22] has been investigated for coastal regions. Experimental data were also conducted over a 3 year period to investigate the impact of the variation of the aerodynamic roughness length over heterogeneous surfaces using roughness elements such as vegetation height and the leaf area index [23] Further research addressing the analysis of the wind potential in both limited regions as the canary Islands [24] and worldwide [25], selected the values of the roughness from tables and used these for extrapolating the wind speed from the measurement height to the hub height of the WT based on the land cover surrounding a given location derived by satellite images.

With the increase of the quality of spatial data, GIS has been widely used to estimate the potential of RES in large regions: wind, solar and biomass resources and potential are usually the topics addressed and about which many studies have been done in the last decade. Studies in the field of wind energy aimed at carrying out statistical analyses of the distribution of wind farms in China [26] or at defining suitable regions for wind energy projects in large regions such as Tuscany [27] and Switzerland [28] demonstrated the flexibility of GIS platforms. GIS software was also used to carry out technical and economic analysis of exploitable lands in Iowa [29] and showing the impact of the PPA on the change of the rate of exploitation of a land. In the field of energy policy, GIS has been used to investigate the effect of different policies to support wind energy projects [30] in Brazil. A few research studies addressed the issue of estimating the wind AEP in a given location using technical specifications of wind characteristics. For example, GIS software was combined with additional commercial tools for estimating the AEP [31] of 5 WTs of a potential wind farm located on the island of Lesvos in Greece. The proposed process coupled Wind Atlas Analysis and Application Program (WAsP), to estimate the regional wind resource, with a GIS platform to identify the site. Nevertheless the process did not take into account the wake effect and the different elevation of the WTs when estimating the AEP. Similar studies aimed at estimating the potential of wind energy potential in India [32], in China [33], on Spanish islands [34], and in Poland [35] with GIS calculated the AEP of potential wind farms on suitable land assuming a regular layout and fixed operating parameters of wind farms such as constant array losses, annual availability, grid availability factor and transmission losses.

The analysis of the roughness factor is fundamental in order to determine the parameters of the wind speed (e.g., the Weibull parameters) when extrapolating at the hub height of the WTs. These parameters are usually automatically calculated with commercial tools such as WaSP[1] or, as mentioned before, mean annual values for roughness values are conjectured independent of the wind direction. Terrain roughness has been studied at different scales and using different methods in order to describe the friction of the terrain on the wind profile, also using wind speed measurements at different heights. In order to estimate the AEP, some assumptions related to the micro-siting are set, such as the mean theoretical annual roughness factor based on the tables derived by satellite images such as CORINE [36] (when wind measurements at different heights are not available) and the losses due to the WTs array.

GIS technology has been widely applied in multiple fields from spatial modeling and planning in domains such as economy, social science, planning to physical modeling such as hydrology. In the wind energy field, no study has yet demonstrated the ability of GIS when estimating the wind energy generation of wind turbines including the effect of the roughness and the interaction of WTs that generates wakes and thus losses. Most of these analyses are carried out with commercial tools which are not based on GIS technology.

The aim of our work is to demonstrate that GIS tools enable the modeling, in a unique workflow, of the roughness factor and the

---

[1] http://www.wasp.dk/.

integration of physical models of wake effects resulting from the interaction among WTs. The roughness factor changes as a function of the wind direction at a given site of a wind energy project and for each wind turbine in particular in locations where nearby the land cover is irregular. The time period over a year also implies different characteristics of the land cover and thus of the roughness factor that have to be taken into account. The integration of physical models such as the wake effects is the other challenge presented in this paper as it takes into account both the spatial variation of the roughness and the difference in the elevation of the WTs sparsely located in a given region. In previous work only two-dimensional problems have been addressed, while in this research, in addition to the variation of the elevation, that shifts the modeling into a three-dimensional problem, the modeling of the overlapping areas of wakes of each WT for each wind direction is addressed. The model presented here shows that complex physical modeling embedded in dedicated tools can be also implemented in a GIS platform which is suitable both for large-scale analysis and local assessments. This process will be evaluated by comparing the actual AEP of four wind parks in Kansas (U.S.) to the predictions. In addition, the uncertainties will be quantified. Moreover the influence of the WTs layout on the AEP is quantified by introducing a coefficient that shows the reduced energy production as function of the variation of the wind direction.

3. Methodology

The workflow adopted in this work comprises four main steps: (1) data selection and creation of a geodatabase, (2) modeling of the terrain roughness, (3) modeling of the wake effect due to the interaction of WTs, (4) estimation of the AEP and the quantification of its uncertainties and (5) assessment of the reduced energy production due to the wind farm layout and the variation of the wind direction. These steps are described in detail in the next sections.

The state of Kansas is located in the central part of the Midwest of the United States; this region encompasses the area from the Great Lakes to the Rocky Mountains and from North Dakota to Texas. The region is also characterized by the highest exploitable wind energy potential in the U.S. according to NREL. Kansas has a low population density mostly concentrated in a few main cities. Like the other states of the Midwest, most of the land is used for agriculture and its topography is composed of flat terrain and rolling hills in the central-eastern region and low mountains in western region. Elevation ranges between 207 m and 1232 m ASL.

NREL estimates that Kansas has the 2nd largest exploitable wind resource potential after Texas [37]. The wind resource is mainly concentrated in the central-western region with average annual wind speed higher than 8.5 m/s at 100 m AGL[2]. Most of the operating wind energy projects are also located in these regions, for an overall installed capacity of 2'611 MW at the end of 2012[3].

3.1. Data and software

The first stage of this work is concerned with the selection of the GIS data that describe the land features in vector and raster format. Data such as land cover, administrative boundaries, linear infrastructures, water bodies, protected areas, DEM and topographic maps are provided by the Kansas Data Access and Support Center[4] (DASC). The selected DEM has a 10 m resolution.

Wind data in GIS format are obtained using a Mesomap system consisting of an integrated set of atmospheric simulation models, databases, and computers and storage systems. At the core of Mesomap is MASS (Mesoscale Atmospheric Simulation System), a numerical weather model, which simulates the physics of the atmosphere using long-term wind speed measurements. These data is provided both in raster and vector format. Vector data (shapefile with points), containing the necessary wind data, are used in this study. The wind speed data characteristics have a resolution of 2.5 km and are simulated for all 16 sectors in which the wind rose is divided (Fig. 1). For each sector, data such as mean annual wind speed, Weibull parameters, and power density at 50 m AGL are provided.

The location of the wind turbines in shapefile format (points) are available at the DASC webpage and verified using Google Earth.

The data required to describe the terrain roughness at a given wind farm site are collected in a geodatabase by an automated process described in detail in the next sections. The developed process is realized with ArcMap 10 of the Environmental Systems Research Institute (ESRI[5]) ArcGIS software package. ArcGIS provides multiple geoprocessing tools for vector and raster data that allow the creating of complex workflows and provides extensive libraries and geoprocessing modules to build powerful scripts. Model Builder is then used to create the workflow.

3.2. Characterization of the terrain roughness and ruggedness

In this stage, a process that models the variation of the terrain roughness over the year has been developed. It is composed of three main sub-steps: a pre-processing phase, the estimate of the roughness and ruggedness (main process) and the generation of the attribute data containing all the calculated data. The calculated data are appended to the attribute data of the shapefile representing the locations of the WTs.

The terrain roughness factor z_0 describes the land characteristics and is used as input factor to extrapolate the wind speed from the measurement heights to the hub height. The extrapolation of the wind speed to the hub height is carried out with the following formula [38]:

$$\bar{u}_H = \bar{u}_{\text{ref}} * \ln\frac{H}{z_0} / \ln\frac{H_{\text{ref}}}{z_0} \qquad (1)$$

Multiple studies have been conducted to define the value of z_0 [39,40] and show how the wind shear exponent, that depends on the roughness, changes with the wind direction [41]. The values of z_0 used in this work are reported in Table 1. As the land cover changes over the year, the z_0 value also changes over the year; for this reason, we conjectured the characteristics of the land cover in Kansas over the year in order to estimate a more realistic value of the terrain roughness.

We considered on the one hand the fact that the ground is covered with snow for a few months and, on the other hand that those areas used for crop farming are characterized by a different land cover in the summer. The intermediate steps of the vegetation growth are also taken into account. This process is modeled and twelve different raster data sets corresponding to each month are created to describe the land cover change over the year. For each WT position, each n sector is assigned a monthly z_0 (Fig. 2).

In addition the ruggedness of the terrain is calculated. The ruggedness index (RIX) is a parameter that describes the complexity of the topography of a given region that is steeper than a certain critical slope (18°) in a circular area of a 7'000 m diameter. If RIX exceeds 30%, the terrain is considered complex [42,43]. The
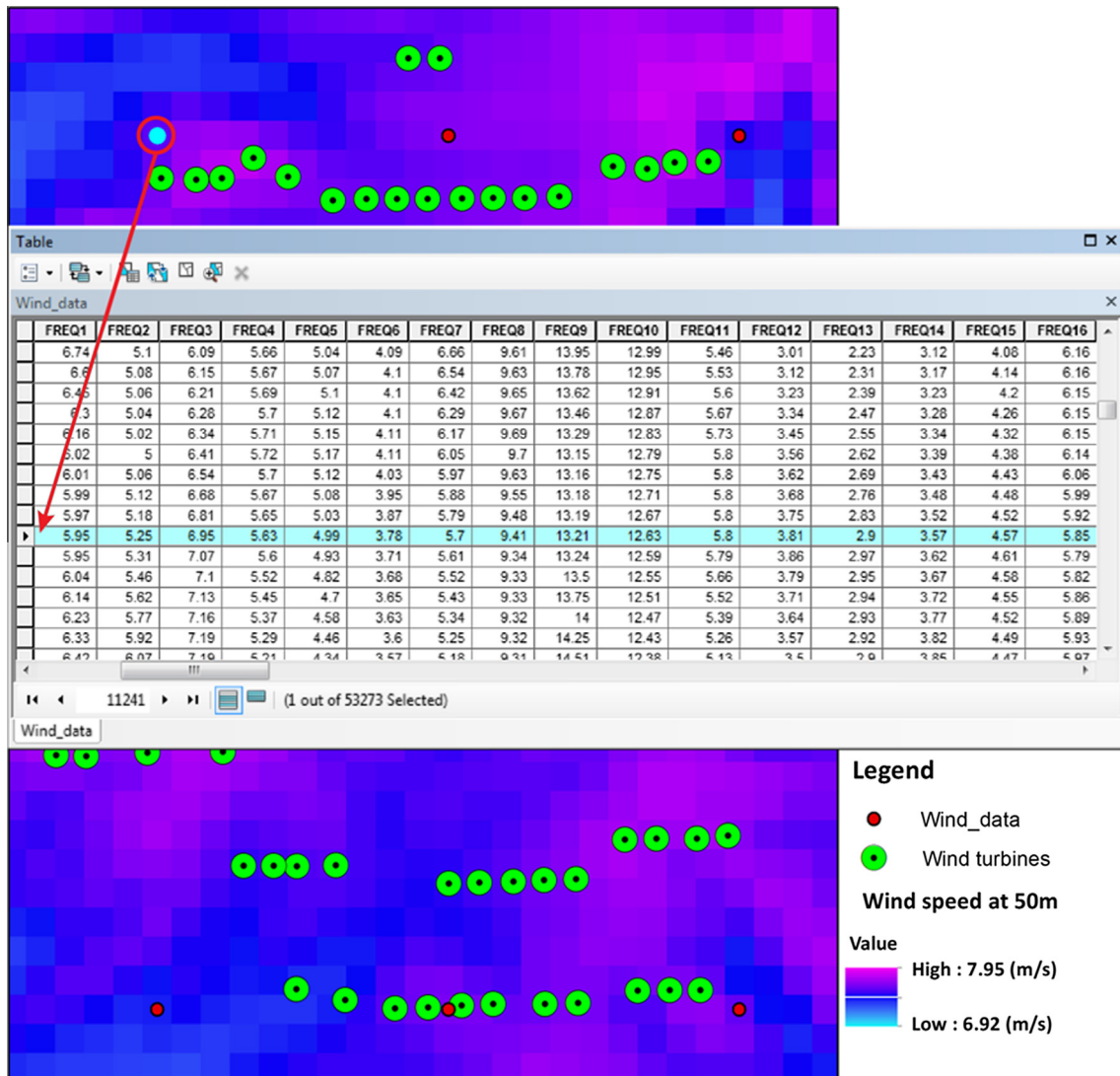
Fig. 1. Excerpt of the distribution of wind speed points with the data of 16 sectors. In the table, the frequency of the wind direction is highlighted with blue color. (For interpretation of the references to colour in this figure legend, the reader is referred to the web version of this article.)

developed process is designed to assess the AEP also for complex terrain, thus this parameter will be taken into account. The ruggedness index has been also used in previous work in order to improve the wind power prediction in complex terrain [44]. The analysis of heterogeneity of the terrain is carried out with GIS software using the DEM as demonstrated in previous studies [45].

The RIX is calculated using the Raster Algebra function available in ArcMap with the following formula:

$$RIX = n_{30}/n_{all} \tag{2}$$

In case of the measured wind speed data are provided by a mast, a ΔRIX is calculated showing the uncertainties when estimating the AEP of WTs.

Then the ΔRIX [44] is calculated:

$$\Delta RIX = RIX_{wt} - RIX_m \tag{3}$$

where RIX_{wt} is the ruggedness around the WT_i, and RIX_m is the ruggedness around the meteorological mast.

If: ΔRIX < 0, then the estimated wind speed is underpredicted. ΔRIX > 0, then the estimated wind speed is overpredicted.

This parameter is calculated if the wind speed observations are not located at the wind energy project site and thus used to adjust

the prediction of the AEP [42]. For the case studies presented in this paper, the value of the ΔRIX is zero because of the long-term estimated wind data measurements are in a dense regular grid that are close to the WT locations. Therefore the ΔRIX value has no impact on the estimate of the AEP.

The monthly and annual values of z_0 and the parameters RIX and ΔRIX are estimated for each sector, by which the wind rose is divided. The main process is made up of three steps in which workflows and subroutines are developed in order to define the before-mentioned parameters. The computational time depends on the number of WTs included and the raster data resolution: for the four case studies it is comprised between 24 and 36 h.

In the final step the outcome of the computation is added to the attribute table of the shapefile of the WT data points. In addition, other data, such as the altitude of the WTs, the geographic coordinates (X_i, Y_i), the rotor diameter and the hub height, are also included.

3.3. Wake model

The electricity generated by a wind energy project is a function of a complex interaction of the WTs and in particular dependent on the generated wake effect, when the wind flows through the

Table 1
Roughness length scale table.

Land cover classes	Roughness z_0
Lake, sea	0.0001
River	0.0003
Marsh/swamps	0.0005
Bare rock; rubble; pebbles	0.005
Bushes/undergrowth (sparse)	0.016
Lawn	0.02
Natural grassland; pastures	0.04
Vineyard	0.1
Orchard	0.3
Continuous urban fabric	0.5
Bushes/undergrowth (dense)	0.6
Forest (sparse)	0.6
Forest; mixed forest	1
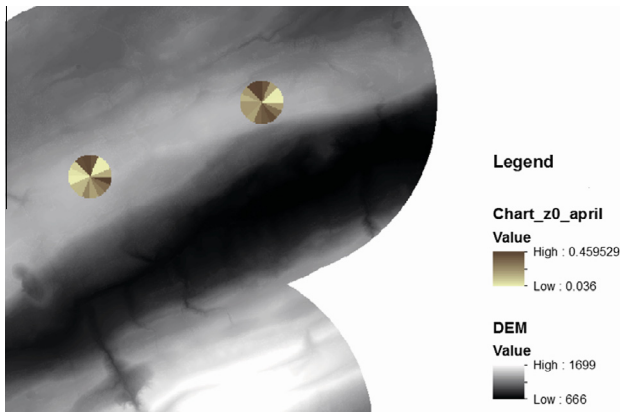
Fig. 2. Example of representation of the roughness value z_0 for each WT location in April.

blades. The data contained in the attribute table of the shapefile of the WTs are used.

The process is described in discrete steps. Assuming that the wind rose is divided into n sectors (corresponding to n different wind directions), the wake effect and all parameters necessary to estimate the AEP are evaluated n times.

For each sector, the coordinate system of the WTs is adapted in a way that the positive x-axis is aligned with the wind direction. Assuming that the actual coordinates of the WTs are fixed (x_i, y_i), a new set of coordinates (X_i, Y_i) is calculated for each sector with the following formula:

$$\begin{vmatrix} X_i \\ Y_i \end{vmatrix} = \begin{vmatrix} \cos(\varphi + 90) & \sin(\varphi + 90) \\ -\sin(\varphi + 90) & \cos(\varphi + 90) \end{vmatrix} \begin{vmatrix} x_i \\ y_i \end{vmatrix} \qquad (4)$$

For each n direction, the relative distance of the WTs is calculated in its x_i and y_i components.

The location of the WTs is such that the wake generated by a WT_i in upstream can influence a WT_k in downstream depending on the relative position of the WTs and the wind direction ϕ. For this reason, when the coordinates of each WT are calculated for each wind direction ϕ, the overlapping area of the wakes on the rotor of the WTs in downstream is also calculated.

The WTs are then ranked according to their x value (corresponding to the wind direction) in order to identify which WT is in upstream position in respect to the other WTs. The WT that is hit first by the wind is assigned the value 1 and the last one is assigned the number N corresponding to the total number of WT forming the wind farm. The rank changes for each wind direction and it is used at each loop to identify in which sequence the WTs have to be selected when estimating the AEP.

A process is designed to identify whether a WT_k in downstream is completely in the wake, partially in the wake or not in the wake: each WT is assigned a value that defines one of the three conditions:

$0 = WT_k$ not in the wake

$1 = WT_k$ partially in the wake

$2 = WT_k$ completely in the wake

The reciprocal distance between WT_k and WT_i is assessed with the relations:

$$\Delta LD_{ik} = X_i - X_k \quad \Delta HD_{ik} = Y_i - Y_k \qquad (5)$$

There is influence between a WT_k and the approaching wake if:

$$LD_{ik} < 0 \ \& \ 3Ddist_{ik} + D/2 \le DW_{ik} \qquad (6)$$

where: $3Dist_{ik} = \sqrt{\Delta HD_{ik}^2 + \Delta z_{øik}^2}$

If the rotor of the WT_k in downstream is completely in the wake then

$$A_0 = A_k = \pi(D/4)^2 \qquad (7)$$

where A_0 is the overlapping area between the wake generated by the WT_i and the rotor of the WT_k in downstream.

If the rotor of the WT_k in downstream is partially in the wake (Fig. 3) then

$$A_0 = r_k^2 \cos^{-1}(d^2 + r_k^2 - r_i^2/2dr_k) + r_i^2 \cos^{-1}(d^2 + r_i^2 - r_k^2/2dr_i)$$
$$- \frac{1}{2}\sqrt{(-d + r_k + r_i)(d + r_k - r_i)(d - r_k + r_i)(d + r_k + r_i)} \qquad (8)$$

In case of partial overlap of the wake with the rotor of a WT_k in downstream, the inlet velocity is calculated using the following relation:

$$\bar{u}_k = \bar{u}_i - \sqrt{\sum_m (A_0/A_i) * (\bar{u}_i - \bar{u}_{ik})^2} \qquad (9)$$

The wake model adopted in this work is from Frandsen et al. [46] and takes into account the thrust coefficient and the power output of the WT.

The growth of the wake behind a WT_i is calculated with the following formula:

$$D_{i\text{-wake}} = D_i(\beta \exp(k/2) + \alpha\lambda) \exp(1/k) \qquad (10)$$

where $\lambda = x/D_i$

$D_{i\text{-wake}}$ is the diameter of the wake at the distance x in downstream of the WT_i as shown in Fig. 3.

The factor α is the constant characteristic of the wake expansion [46] and it is calculated with the following formula:

$$\alpha = 0.5/\ln(H/z_0) \qquad (11)$$

The wind speed in the wake is described by [46]

$$\bar{u} = (1/2 + 1/2\sqrt{(1 - 2C_t(A/A_w))}) \qquad (12)$$

The power coefficient and the thrust coefficient are related through the following relation:

$$C_p = 4a(a - 1)^2 \qquad (13)$$

And the induction factor and the thrust coefficient are related by the following relation:

$$a = 1 - \sqrt{1 - C_t} \qquad (14)$$

3.4. Estimate of the AEP

As the data of the wind speed characteristics used in our process are assessed at 50 m height and the hub heights of the current
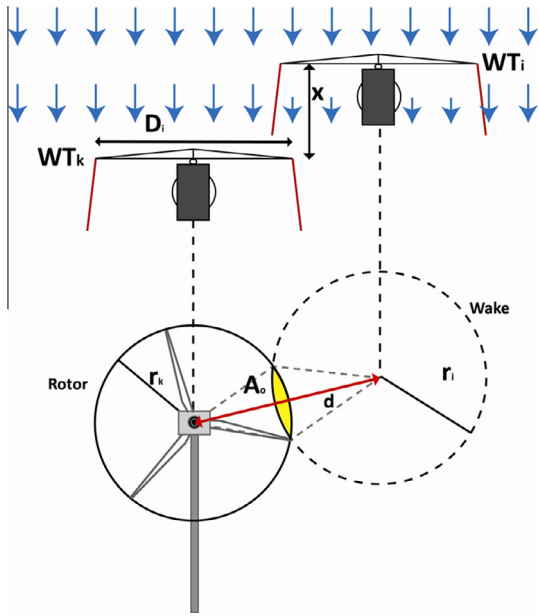
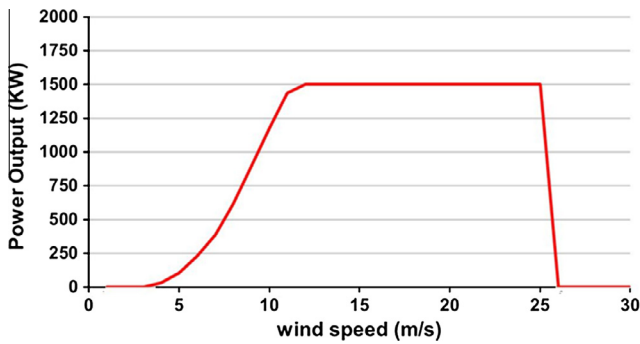**Fig. 3.** Overlapping area between the rotor and the wake.

Fig. 4. Power curve of a 1.5 MW WT.

WT models are higher, an extrapolation is required. The wind speed is extrapolated using Eq. (1), whereas the Weibull parameters required for estimating the AEP are extrapolated using the following formulas that have been widely applied in other work [15,47,48]:

$$k_a = k_{ref} / \left[1 - 0.0881 \ln \frac{H}{H_{ref}} \right] \tag{15}$$

$$C_a = C_{ref} (H/H_{ref})^n \tag{16}$$

$$n = [0.37 - 0.0881 \ln C_{ref}] / \left[1 - 0.088 \ln \frac{H_{ref}}{10} \right] \tag{17}$$

The estimate of the AEP is carried out using the power curve of a wind turbine. The power curve (Fig. 4) is split into two sections:

$P = 0$	$if \, \bar{u} < u_{\text{cut-in}}$
$P = 5\text{th order polynomial}$	$if \, u_{\text{cut-in}} \leq \bar{u} \leq u_{\text{rated}}$
$P = \text{cost}$	$if \, u_{\text{rated}} < \bar{u} < u_{\text{cut-off}}$

where $u_{\text{cut-in}}$ is usually set at 3–4 m/s, u_{rated} is usually set in the range of 12–14 m/s, and $u_{\text{cut-off}}$ is usually set at 22–25 m/s.

The 5th order polynomial interpolates the points of the selected WT power curve. The power curve is provided by the WT manufacturer at an air density of 1.225 kg/m³. The $u_{\text{cut-in,}}$ u_{rated} and $u_{\text{cut-off}}$.
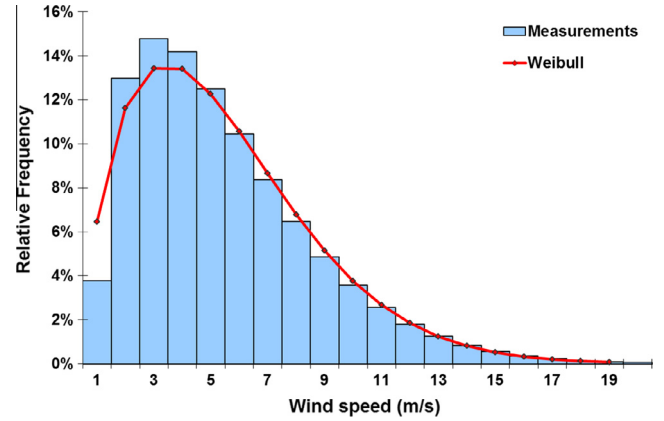

Fig. 5. Weibull distribution of the wind speed.

For each WT the AEP is calculated by applying the method of bins [49]: for each bin (e.g., 1 m/s) of the probability distribution of wind speed (Weibull curve) (Fig. 5) described by the following relation (Eq. (15)), the frequency $\mu(u)$ and the power output of the wind speed u are used to estimate the AEP (Eq. (16)) of each WT:

$$\mu(\bar{u}) = (k/C)(\bar{u}/C)^{k-1} \exp(-(\bar{u}/C)^k) \tag{18}$$

$$\text{AEP}(\text{WT}_n) = 8760 \gamma_{\text{avail}} \varepsilon_{\text{loss}} \sum\nolimits_{\text{cut-in}}^{\text{cut-off}} \sum\nolimits_n \mu(\bar{u}) P(\bar{u}) \tag{19}$$

The availability γ of the WTs has been set at 97% with an annual decay of the performances of 0.5%.Other losses ε such as mechanical and electrical losses are also included in the model and set at 1.5%.The estimate of the AEP of the entire wind farm is the sum of the AEP of all WTs.

$$\text{AEP}_{\text{tot}} = \sum\nolimits_j \text{AEP}(\text{WT}_j) \tag{20}$$

The dots in Fig. 6 represent the positions of the WTs of one of the case studies and their sizes are proportional to the estimated AEP. It can be seen that the WTs that generate the highest AEP are located in the lower front part of the wind farm. This is due to the prevailing wind direction blowing from South–South-West (Fig. 6) and the topography as it can be seen in Fig. 7. The WTs represented by small dots generate a lower AEP because of the wake effects of the other WTs, even where the wind speed is higher than in locations where WTs generate more electricity. In the attribute table in Fig. 6, the average predicted AEP (red circle), the k and C factors (blue and green rectangles) of the Weibull distribution calculated at 50 m AGL are shown: these are the values corresponding to the WT highlighted with the blue spot. For each WT the same parameters are assigned.

3.5. Impact of wake effect on annual energy production

As the WTs within a wind farm interact by shadowing each other and thus reducing the inlet wind speed, the AEP of each WT is affected by the wind direction, its corresponding wind speed distribution and the layout of the other WTs. Usually wind farms are designed in order to maximize the extraction of energy from wind but, as the wind direction changes, usually prevailing wind direction is selected as one of the fundamental parameters to set the layout. An incorrect analysis of the wind resource can result in a not optimized layout that can generate therefore significant energy losses increase the turbulence overloading the WTs and affect the cash flow of the project. In order to identify the impact of the layout, and the generated wakes, on the AEP of a wind farm, a coefficient called "reduced efficiency coefficient" (REC) for each wind direction has been defined as:
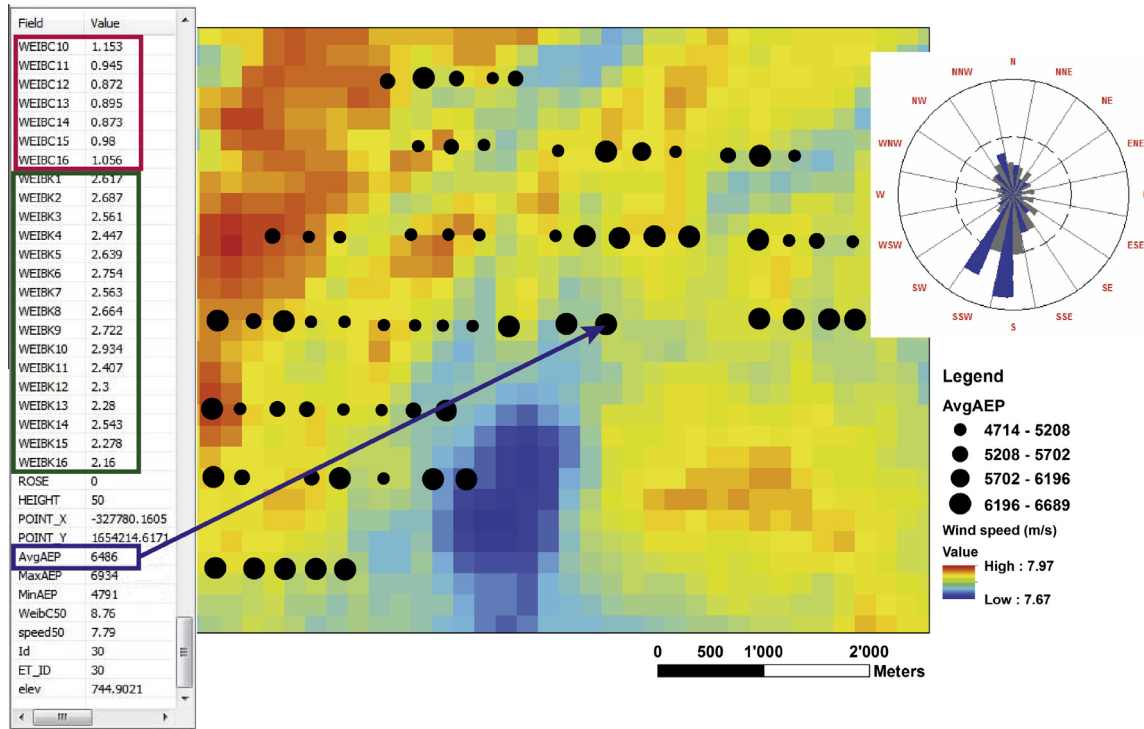
Fig. 6. Representation of the layout of the WTs with circles proportional to the estimated AEP (MWh).
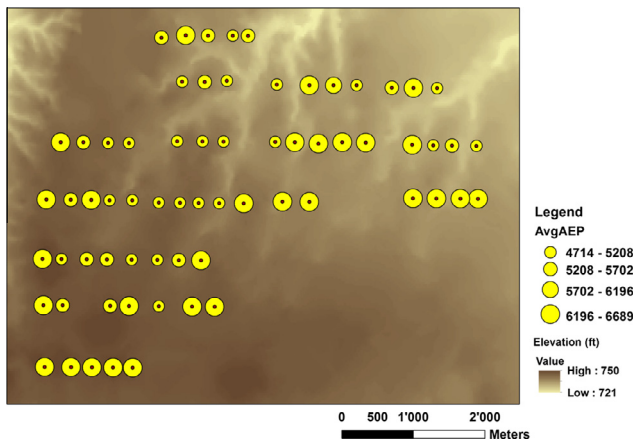

Fig. 7. Layout of WTs with respect to topography; the internal dark spot of each circle is the location of each WT.

$$REC^{\varphi} = \left(AEP^{\varphi}_{ww} / AEP^{\varphi}_{w/w} \right) - 1 \tag{21}$$

It is a negative number comprised between 0 and −1 that shows how the AEP of a given WF layout is reduced due to wake effect when the wind blows from a direction φ compared to an ideal situation where the wake effect is neglected when estimating the AEP. The lower the REC is, the greater is the impact of the wake on the AEP. In this work, four different wind farms are used to show the reduction of the AEP over the 16 wind directions by which the wind rose has been divided.

4. Results and discussion

We tested and evaluated the developed process with four case studies. The mean actual AEP of each wind farm was compared to the estimated AEP and then the uncertainties were assessed.

The selected wind farms are composed of an overall number of 377 WTs for an overall rated installed capacity of 462 MW whose range of operating years is between 2 and 11. The WT models have a rated power output between 660 kW and 2.5 MW.

The location of the selected wind farms are shown in the map below (Fig. 8).

The actual AEP of the selected wind farms is issued by the EIA-DOE. For each case study the ability to assess the uncertainties when predicting the AEP is carried out using the following formula:

$$\Delta = \left(AEP_{predicted} / AEP_{actual} \right) - 1 \tag{22}$$

A positive value of Δ indicates an overestimate of the AEP, whereas a negative value indicates an underestimate.

Fig. 9 shows the comparison of the actual and the predicted AEP. The dots represent the actual AEP of the four wind farms, whereas the continuous line represents the average value of the predicted AEP.

The comparison of the long-term predicted to the actual AEP shows on average an underestimate of the AEP of the four case studies by 3.56% with a standard deviation σ is 5.21%.

In Table 2 the estimated capacity factor is compared to the actual one; the extreme values are an overestimation of 1.11% and an underestimation of 4.28%.

The REC has been estimated for all wind farms and the results are shown below. The x-axes show the number of sectors in which the wind direction is divided: the sector n.1 corresponds to the wind blowing to North and each increasing number corresponds to the following sector in clockwise direction. The y-axes show the REC corresponding to each wind direction (or sector).

For all wind farms the wind direction with the lowest REC and thus most inefficient energy extraction is when the wind blows from East (sector n.13) and from West (sector n.5). This is due to the fact that the WTs are placed in line and not far away from each other along the direction East–West. This is due also to the fact the
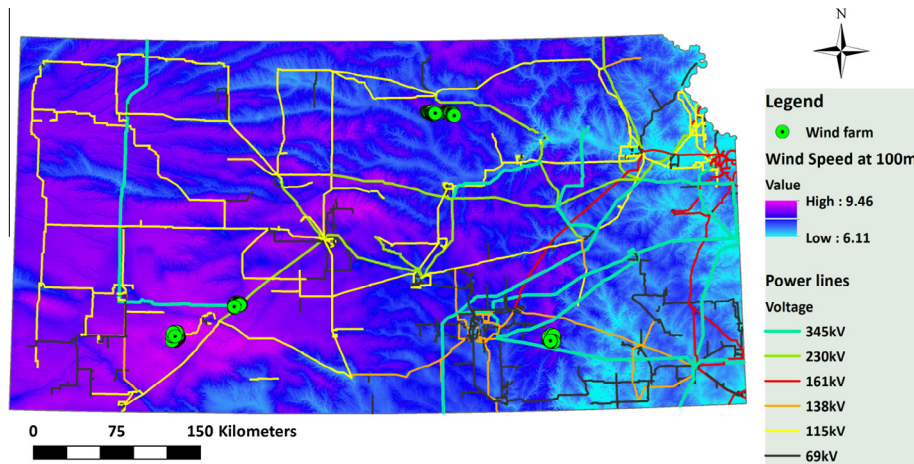
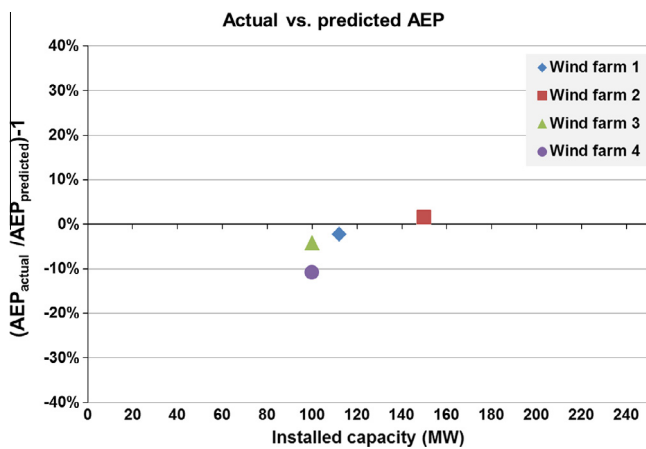**Fig. 8.** Location of the 4 case studies in Kansas.

Fig. 9. Comparison of the actual AEP vs. the predicted AEP for the 4 case studies.

prevailing wind direction (towards North and North-East) is used to set the layout of the WTs and to maximize the energy extraction from this direction. This can be clearly seen at the sector n.8, n.9 and n10 corresponding to the wind direction blowing in the direction of North and North-East (Fig. 10).

On average the REC of each individual wind farm is comprised between −0.087 and −0.2. Looking at the single sector, an average REC value equal to −0.44 corresponds to the n.5 while the best performing sector is the n.10 with an average REC value equal to −0.07. The worst performance is achieve by the wind farm n.2 with a REC equal to −0.62 while the best one is achieve by the wind farm n.4 at the first sector with a REC value of −0.02.

In previous studies where the AEP of WTs was estimated with GIS, the main assumption was to consider a specific regular layout of WTs in order to minimize their interaction. The loss of energy production due to the wake effect in case of a regular layout is a function of the spacing as discussed in [24,50] and it varies from around 50% to 96% respectively for a 10 × 10 WT grid and 4D spacing along the main wind direction. Also Hossain in [32] used very similar assumptions to estimate the AEP of wind turbines assuming a specific layout and neglecting the different heights of rotors due to the irregularity of the terrain. In [35] the estimated full load hours are higher than the measured one because the wake effect is not included and thus a parameter ranging from 0.83 to 0.9 has to be applied to the full load hours. Also in this study a 6D × 6D regular layout is assumed to smooth the losses due to the interaction among WTs. For the modeling of on-shore technical wind energy potential in Spain [51], a 8D × 8D spacing is considered for each suitable land. Nevertheless the wake effect itself was not specifically integrated in GIS models and the loss at each specific wind direction not calculated. Previous studies demonstrated how the wake effect has an important impact on the estimate of the electricity generation of clustered WTs, but in GIS modeling this is simplified by multiplying the estimated full load energy production with a constant parameter. This constant parameter is a function of the number of WTs assumed to be regular. In reality the wake effect is a combination of multiple factors such as wind regime, WT characteristics, topography, relative height difference of WTs within a wind farm, relative distance among WTs which are usually set in an irregular layout, and the roughness which affects the wind profile. This 3-dimensional aspect combined with the variation of the wind direction and the layout of the WTs has an influence on the reciprocal shadowing of WTs and thus on the energy generation. Therefore the losses due to wake effect, difference in elevation and the variation of the wind direction are unlikely to be modeled or precisely accounted for by a generalized standard energy loss factor due to a given regular array or layout.

As the aerodynamic roughness factor is demonstrated to have an impact on the wind profile, in this work it has been estimated for each sector in which the wind rose is divided. In [52] the roughness factor is assumed to be constant for the all areas around potential or existing wind energy projects or simply assigned to each cell of the land cover [29,32,35] independent from the wind direction. This is a simplification of the spatio-temporal variation of the roughness factor to extrapolate wind speed from measurement height (usually lower than 50 m AGL) to the hub height for a given wind direction. In this study, we want to demonstrate that with a GIS tool, the roughness factor around each WT can be assessed and associated to each sector to extrapolate the wind speed to the hub height as a function of the wind direction. In the four case studies used in this work, the wake effect generates losses ranging from 8.7% to 20% for wind farms characterized by

Table 2
Comparison of the actual vs. predicted capacity factor (CF).

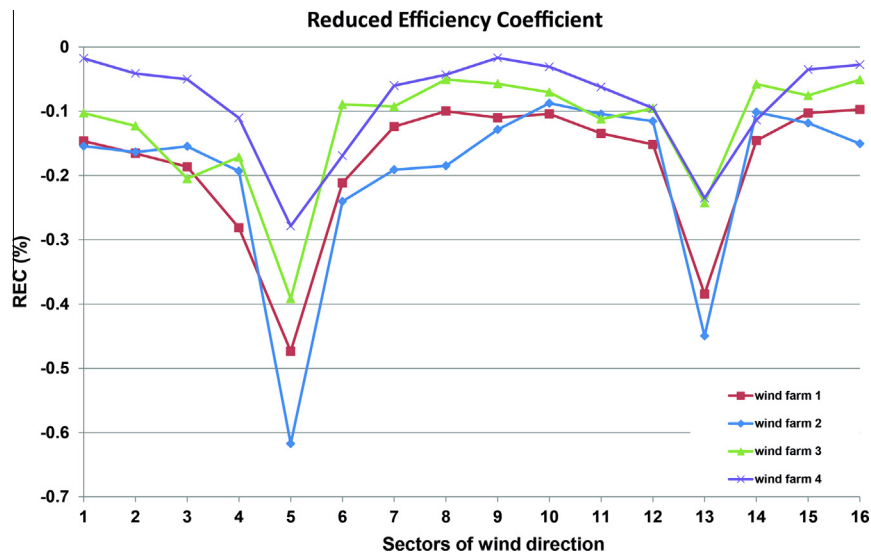| Kansas	Long term CF		
	Actual CF (%)	Predicted CF (%)	Δ (%)
Wind farm 1	36.90	35.71	−0.89
Wind farm 2	41.77	42.38	0.61
Wind farm 3	39.67	40.21	0.55
Wind farm 4	43.40	38.67	−4.73

Fig. 10. Distribution of the REC as function of the variation of the wind speed direction.

both relatively regular and irregular layouts. As the number and the size of WT[6] change depending on multiple local boundary conditions due to land and wind resource characteristics, the application of constant parameters to take into account the losses due to the wake effect seems a coarse simplification to overcome the issue. The proposed methodology can be easily integrated in each large-scale model to estimate the AEP for any type of wind farm layout that can be identified in any buildable land. For any type of wind farm layout, the model only requires, as input parameters, the geographical location of the WTs, their technical characteristics, the features of the surroundings such as land cover and digital terrain model and the spatial distribution of the characteristics.

5. Conclusion

In this work we presented a GIS-based process to estimate the AEP of clustered WTs. The process models for each sector n of the wind rose the monthly variation of the terrain roughness, assesses the RIX factor and takes into account the interaction of the WTs due to the wake effect. The work demonstrates that the wake effect due to the interaction of multiple WTs and the analysis of the roughness factor depending on the wind direction can be modeled and embedded into a GIS-based process. In addition, in comparison to previous work, the spatial distribution of the wind speed data includes also the wind characteristics as a function of the wind direction. This enables a more realistic modeling of the actual conditions and thus a more reliable assessment of the long-term AEP of a wind farm instead of posing multiple hypotheses (e.g., the losses due to the wake effect as a function of a fixed percentage of the AEP independent from the WT layout, a unique roughness value independent from the wind direction, etc.). The difference in the elevation of the WTs composing a wind farm has been modeled as it affects the shadowing of WTs as a function of the variation of the wind direction.

The model was tested comparing the predicted AEP with the actual AEP of four wind energy projects. Results showed an overall underprediction of the AEP of 3.56% and an underprediction of the long-term CF of 1.11%.

The reduced efficiency coefficient has been introduced to assess the performance of the layout of the wind farms in respect to the wind direction and the wind speed distribution. The wind farms show an average REC of −0.15 with extreme values equal to −0.2 and −0.087.

The results are very encouraging and demonstrate that the uncertainties of the AEP prediction in case of flat or hilly terrain are low. The developed process can be used in the wind energy industry and customized models for estimating the AEP can be developed using a GIS-based platform in order to achieve optimal performance.

Future development of the process should address the analysis of wind farms in the presence of complex conditions (e.g., complex topography and forests): this aspect could not be investigated in the State of Kansas because the topography of the locations around the existing wind farms is characterized by relatively uniform and similar conditions. For this purpose other regions have to be identified and analyzed in specific studies, where existing wind energy projects are located in regions with the searched characteristics. This is one of the fundamental future aspects to be investigated in order to assess the reliability of the proposed tool: the influence of the complex topography combined with the spatio-temporal variation of the land cover (e.g., forest or patchy vegetation and settlements) play an important role in the extrapolation of the wind speed to the hub height. Additional implementations concern the use of wind speed measurements of remote met stations to estimate the AEP of a wind farm and the comparison of the performance of other wake models integrated in the GIS model.

Economic and financial parameters should be also included for the assessment of economic feasibility. This would enable a complete analysis of wind energy projects over large regions.

Other potential work should address the development of a GIS-based workflow that optimizes the positions of WTs under realistic conditions such as topography, parcel distribution and setbacks from roads and buildings. Previous research studies focused on the optimization of WTs considering flat terrain, a prevailing wind direction and little other constraints that usually have an impact on the layout of wind energy projects.

Significant efforts should also be made concerning the assessment of the spatial distribution of the wind resource. The assessment of the wind energy potential at any scale in a given region is presently strongly dependent on the availability of the spatial distribution of the wind characteristics in GIS compatible format with the corresponding spatial uncertainty. These data are currently created using mesoscale models described in Section 2. This

---

[6] http://www.wwindea.org/home/index.php.

aspect somehow limits and slows down the use of GIS and further detailed analyses aimed at assessing the spatial uncertainties of the potential. In particular, as wind resource is a spatio-temporal stochastic resource, the estimate of the spatial uncertainties around the mean values would enable a more detailed risk analysis. As GIS allows for integration of geostatistical and physical models and processes, future work should focus on the development of a GIS-based method aimed at creating wind speed maps with their spatial uncertainties. This will enable to overcome the issue of using different software and thus to embed in a unique package processes from the assessment of the wind resource at large scale to the optimal siting of WTs in limited areas.

References

[1] REN21. Renewables 2012 Global Status Report. Paris; 2012.
[2] Gsänger S, Pitteloud JD. World Wind Energy Association WWEA 2012. Bonn, Germany; 2012.
[3] Lei M, Shiyan L, Chuanwen J, et al. A review on the forecasting of wind speed and generated power. Renew Sustain Energy Rev 2009;13:915–20.
[4] Foley AM, Leahy PG, Marvuglia A, et al. Current methods and advances in forecasting of wind power generation. Renew Energy 2012;37:1–8.
[5] Stathopoulos C, Kaperoni A, Galanis G, et al. Wind power prediction based on numerical and statistical models. J Wind Eng Ind Aerodynam 2013;112:25–38.
[6] Castro Sayas F, Allan RN. Generation availability assessment of wind farms. IEE Proc-Gener Transm Distrib 1995;143:507–18.
[7] Biswas S, Sraedhar B, Singh Y. Simplified statistical technique for wind turbine energy output estimation. Wind Eng 1995;19:147–55.
[8] Lu L, Yang H, Burnett J. Investigation on wind power potential on Hong Kong islands—an analysis of wind power and wind turbine characteristics. Renew Energy 2002;27:1–12.
[9] Jangamshetti SH, Rau VG. Optimum siting of wind turbine generators. IEEE Trans Energy Convers 2001;16:8–13.
[10] Hau E. The wind resource. Wind turbines – fundamentals, technologies, applications, economics. New York: Springer; 2006. p. 451–83.
[11] Johnson GL. Wind Characteristics. In: Wind energy system. Manhattan, Kansas: Kansas State University; 2006.
[12] IEC. Wind turbines. External conditions. Geneva: IEC; 2005.
[13] Genc A, Erisoglu M, Pekgor A, et al. Estimation of wind power potential using Weibull distribution. Energy Sources 2006;27:809–22.
[14] Pallabazzer R. Previsional estimation of the energy output of windgenerators. Renew Energy 2003;29:413–20.
[15] Ahmed Shata AS, Hanitsch R. Electricity generation and wind potential assessment at Hurghada, Egypt. Renew Energy 2008;33:141–8.
[16] Ucar A, Balo F. Evaluation of wind energy potential and electricity generation at six locations in Turkey. Appl Energy 2009;86:1864–72.
[17] García-Bustamante E, González-Rouco JF, Jiménez PA, et al. A comparison of methodologies for monthly wind energy estimation. Wind Energy 2009;12:640–59.
[18] Matthew AL, Anthony LR, Manwell JF. Uncertainty analysis in wind resource assessment and wind energy production estimation. In: 45th AIAA Aerospace Sciences Meeting and Exhibit, Reno; 2007.
[19] Akpinar EK, Akpinar S. An assessment on seasonal analysis of wind energy characteristics and wind turbine characteristics. Energy Convers Manage 2005;46:1848–67.
[20] Irwin JS. A theoretical variation of the wind profile power-law exponent as a function of the surface roughness and the stability. Atmos Environ 1979;13:191–4.
[21] Gardner AG. A full-scale investigating of roughness surface lengths in inhomogeneous terrain and a comparison of wind prediction models for transitional flow regimes: Texas Tech University; 2004.
[22] Gualtieri G, Secci S. Wind shear coefficients, roughness length and energy yield over coastal locations in Southern Italy. Renew Energy 2011;36:1081–94.
[23] Lu L, Liu S, Xu Z. The characteristics and parameterization of aerodynamic roughness length over heterogeneous surfaces. Adv Atmos Sci 2009;26:180–90.
[24] Schallenberg-Rodriguez J. A methodological review to estimate techno-economical wind energy production. Renew Sustain Energy Rev 2013;21:272–87.
[25] Hoogwijk M, de Vries B, Turkenburg W. Assessment of the global and regional geographical, technical and economic potential of onshore wind energy. Energy Econ 2004;26:889–919.
[26] Deng YC, Yu Z, Liu S. A review on scale and siting of wind farms in China. Wind Energy 2011;14:463–70.
[27] Gualtieri G. Development and application of an integrated wind resource assessment tool for wind farm planning. Int J Renew Energy Res 2012;2:674–85.
[28] Dällenbach F, Schaffner B. Alpine wind harvest – development of information base regarding potential and the necessary technical, legal and socio-economic conditions for expanding wind energy in the alpine space – GIS analysis methodology. Bern: Alpine Windharvest partnership netwotk; 2005.
[29] Grassi S, Chokani N, Abhari R. Large scale technical and economic assessment of wind energy potential with a GIS tool: case study Iowa. Energy Policy 2012;45:58–73.
[30] Dutra R, Szklo A. Assessing long-term incentive programs for implementing wind power in Brazil using GIS rule-based methods. Renew Energy 2008;33:2507–15.
[31] Palaiologou P, Kalabokidis K, Haralambopoulos D, et al. Wind characteristics and mapping for power production in the Island of Lesvos, Greece. Comput Geosci 2011;37:962–72.
[32] Hossain J, Sinha V, Kishore VVN. A GIS based assessment of potential for windfarms in India. Renew Energy 2011;36:3257–67.
[33] Zhou Y, Wu WX, Liu GX. Assessment of onshore wind energy resource and wind-generated electricity potential in Jiangsu, China. Energy Procedia 2011;5:418–22.
[34] Schallenberg-Rodríguez J, Notario-del Pino J. Evaluation of on-shore wind techno-economical potential in regions and islands. Appl Energy 2014;124:117–29.
[35] Sliz-Szkliniarz B, Vogt J. GIS-based approach for the evaluation of wind energy potential: a case study for the Kujawsko–Pomorskie Voivodeship. Renew Sustain Energy Rev 2011;15:1696–707.
[36] Silva J, Ribeiro C, Guedes R. Roughness length classification of CORINNE land cover classes. EWEC2007.
[37] Lopez A, Roberts B, Heimiller D, et al. U.S. renewable energy technical potentials: a gis-based analysis. Golden, Colorado: NREL; 2012.
[38] Hau E. The wind resource. In: Wind turbines – fundamentals, technologies, applications, economics. New York: Springer; 2006. p. 462.
[39] Wieringa J. Representative roughness parameters for homogeneous terrain. Bound-Layer Meteorol 1993;63:323–63.
[40] Julieta S, Ribeiro C, Guedes R. Roughness length classification of CORINNE LAND COVER classes. In: Proceedings of the European Wind Energy Conference, Milan, Italy; 2007. p. 7–10.
[41] Ray ML, Rogers AL, McGowan JG. Analysis of wind shear models and trends in different terrain. In: Conference proceedings: American Wind Energy Association Windpower Pittsburgh, PA, USA; 2006.
[42] Mortensen NG, Bowen AJ, Antoniou I. Improving WAsP predictions in (too) complex terrain. In: EWEA proceedings of the 2006 European Wind Energy Conference and Exhibition; 2006.
[43] Bowen AJ, Mortensen NG. Exploring the limits of WAsP: the wind atlas analysis and application program. European Union Wind Energy Conference, Göteborg, Sweden; 1996. p. 584–7.
[44] Mortensen NG, Rathmann O, Tindal A, et al. Field validation of the Δ RIX performance indicator for flow in complex terrain. In: Proceedings of the 2008 European Wind Energy Conference and Exhibition; 2008.
[45] Riley SJ, DeGloria SD, Elliot R. A terrain ruggedness that quantifies topographic heterogeneity. Int J Sci 1999;5:23–7.
[46] Frandsen S, Barthelmie R, Pryor S, et al. Analytical modeling of wind speed deficit in large wind offshore windfarms. WindEnergy 2006;9:39–53.
[47] Justus CG, Hargaves WR, Mikhail A, et al. Methods for estimating wind speed frequency distributions. J Appl Meteorol 1978;17:350–3.
[48] Tar K. Some statistical characteristics of monthly average wind speed at various heights. Renew Sustain Energy Rev 2008;12:1712–24.
[49] Hau E. Power output and energy yield. wind turbines – fundamentals, technologies, applications, economics. Berlin: Springer; 2006. p. 503–5.
[50] Nguyen KQ. Wind energy in Vietnam: resource assessment, development status and future implications. Energy Policy 2007;35:1405–13.
[51] Fueyo N, Sanz Y, Rodrigues M. High resolution modelling of the on-shore technical wind energy potential in Spain. Wind Energy 2010.
[52] Alamdari P, Nematollahi O, Mirhosseini M. Assessment of wind energy in Iran: a review. Renew Sustain Energy Rev 2012;16:836–60.